ANALYTICAL EVALUATION OF THE SECOND ORDER MOMENTUM COMPACTION FACTOR AND COMPARISON WITH MAD RESULTS

J.P. SHAN, S.G. PEGGS, S.A. BOGACZ
Fermi National Accelerator Laboratory*, P.O. Box 500, Batavia, IL 60510

Abstract

The second order momentum compaction factor α_1 is a critical lattice parameter for transition crossing in hadron synchrotrons and for the operation of quasi-isochronous storage rings, which have been proposed for free electron lasers, synchrotron light sources and recently for high luminosity e^+e^- colliders. First the relation between the momentum compaction factor and the dispersion function is established, with the "wiggling effect" included. Then an analytical expression of α_1 is derived for an ideal FODO lattice by solving the differential equation for the dispersion function. A numerical calculation using MAD is performed to show excellent agreement with the analytical result. Finally, a more realistic example, the Fermilab Main Injector, is shown not far away from the ideal lattice.

1 Introduction

In a synchrotron or storage ring, particles with different momenta have different closed orbits. The difference in the closed orbit length (ΔC) between a particle with momentum p and a reference particle with momentum p_0 may be expressed as an expansion in momentum offset δ

$$\Delta C = C_0\alpha_0\delta\left[1+\alpha_1\delta+O(\delta^2)\right]. \quad (1)$$

where C_0 is the length of the reference orbit, and $\delta = \frac{p-p_0}{p_0} = \frac{\Delta p}{p_0}$. Such a dependence of orbit length on momentum is called momentum compaction, and α_0 is the linear momentum compaction factor. The second order momentum compaction factor α_1 is the focus of this paper.

Although rooted in the transverse motion, the momentum compaction effect influences the longitudinal motion through the phase slip factor

$$\eta = \frac{1}{T_0}\frac{T-T_0}{\delta} = \eta_0+\eta_1\delta+O(\delta^2). \quad (2)$$

where $\eta_0 = \alpha_0 - \frac{1}{\gamma^2} \equiv \frac{1}{\gamma_T^2} - \frac{1}{\gamma^2}$, and

$$\eta_1 = \alpha_0\alpha_1 + \frac{3\beta^2}{2\gamma^2} - \frac{\eta_0}{\gamma^2}. \quad (3)$$

Here T is the period of revolution for a particle with momentum offset δ and T_0 is for a synchronous particle, β and γ follow usual relativistic kinematic notation, and γ_T is the transition gamma for a synchronous particle. Near transition η and η_0 are small and the contribution from the nonlinear term $\eta_1 \approx \alpha_0(\alpha_1+\frac{3}{2})$ becomes very important. Nonzero η_1 leads to the fact that higher momentum particles and lower momentum particles can not agree when the synchronous phase should be switched [1], with transition timing spread (the so-called nonlinear time) proportional to $(\alpha_1+\frac{3}{2})$. This intrinsic transition mistiming is partly responsible for longitudinal emittance blow-up and beam loss for some machines. If we can set $\alpha_1 = -1.5$, the nonlinear effect will be suppressed and transition crossing will become much less harmful. For an isochronous electron storage ring, which was proposed for free electron laser [2], synchrotron light source [3] and recently for collider [4], α_1 determines the RF bucket height [5].

2 The Wiggling Factor

The closed orbit $x_{co}(s,\delta)$ of an off-momentum particle is described by the dispersion function

$$D(s,\delta) = \frac{x_{co}(s,\delta)-x_{co}(s,0)}{\delta} = D_0(s)+D_1(s)\delta+O(\delta^2), \quad (4)$$

where $x_{co}(s,0)$ is the reference orbit, and s is the azimuthal coordinate. Furthermore the effect of closed orbit offset on α_1 is negligible [6], therefore we can assume $x_{co}(s,0)=0$. For a span of $d\theta$, the orbit length

$$\begin{aligned} dl &= (\rho+D_0\delta+D_1\delta^2)d\theta\sqrt{1+(D_0'\delta)^2} \\ &= ds\left[1+\frac{D_0}{\rho}\delta+(\frac{D_1}{\rho}+\frac{1}{2}D_0'^2)\delta^2\right], \end{aligned} \quad (5)$$

where $D_0' = \frac{dD_0}{ds}$. This relation is also valid for a straight sector if the limit $\rho\to\infty$ is taken in the appropriate way.

The difference in total closed orbit length of an off-momentum particle from that of a reference particle is simply

$$\Delta C = \oint(dl-ds) = \oint\alpha_0(\delta+\alpha_1\delta^2)ds. \quad (6)$$

Comparison of Eq.(6) and Eq. (6) yields

$$\alpha_0 = \frac{1}{C_0}\oint\frac{D_0}{\rho}ds \equiv \langle\frac{D_0}{\rho}\rangle \quad (7)$$

$$\alpha_1 = \frac{\langle D_1/\rho\rangle}{\alpha_0}+\frac{\langle D_0'^2\rangle}{2\alpha_0}, \quad (8)$$

where $C_0 = \oint ds$ and $\langle\ldots\rangle$ means the average in the whole ring, and the last term in Eq. (8) $w = \frac{1}{2\alpha_0}\langle D_0'^2\rangle = \frac{\langle D_0'^2\rangle}{2\langle D_0/\rho\rangle}$ is called the wiggling factor [7].

Betatron oscillations may also contribute to the difference in orbit length [5], which provides a coupling mechanism between transverse and longitudinal motion. In general, this effect is very small.

3 Differential Equations For The Dispersion Function

The differential equations for dispersion function can be derived from the Hamiltonian, and expanded to the second order of δ

*Operated by the Universities Research Association Inc., under contract with the U.S. Department of Energy.

0-7803-1203-1/93$03.00 © 1993 IEEE

as [6]

$$D_0'' + (\frac{1}{\rho^2} - K_1)D_0 = \frac{1}{\rho}, \quad (9)$$

$$D_1'' + (\frac{1}{\rho^2} - K_1)D_1 = \frac{D_0'^2}{2\rho} - K_1 D_0 - \frac{1}{\rho}\left(1 - \frac{D_0}{\rho}\right)^2 - \frac{1}{2}K_2 D_0^2. \quad (10)$$

where the prime represents the differentiation with respect to s, the azimuthal coordinate. Here $K_1 = \frac{e}{p_0 c}\frac{\partial B_y}{\partial x}$ and $K_2 = \frac{e}{p_0 c}\frac{\partial^2 B_y}{\partial x^2}$ are respectively the quadrupole and the sextupole strength for a reference particle.

These inhomogenous Hill equations could be solved in principle by using Green's function [8]. But it is not obvious to see how the dispersion function is related to other lattice parameters. In the next section we will solve Eq. (9) and Eq. (10) explicitly for an ideal FODO lattice, which is not far away from some realistic lattices, as shown later.

4 A Soluble Case: The Ideal FODO Lattice

The ideal FODO lattice that we consider is composed of N identical FODO cells, or 2N half cells. Each half cell starts at the center of a thin focussing quadrupole (QF) and ends at the center of a neighboring thin defocussing quadrupole (QD). The absolute integrated strength of half QF and QD is the same $q = |K_1|l_{hQ} = \frac{1}{f}$, where K_1 is the quadrupole gradient, and l_{hQ} focal length of the half quadrupole. The bending angle of each dipole is $\theta_0 = \frac{\pi}{N} = \frac{L}{R}$, where L is the half cell length, or the length of each dipole since $l_{hQ} \to 0$, and R is the radius of curvature for the reference particle. Another characteristic parameter is

$$s = qL \approx \sin\phi_{1/2}, \quad (11)$$

which should not be confused with azimuthal coordinate s, where $\phi_{1/2}$ is the betatron phase advance per half cell.

It seems that one only needs to solve Eq.(9) and Eq.(10) in the dipole. Actually the necessary boundary conditions have also to be imposed by the thin quadrupoles.

In the dipole ($\rho = R$ and $K_1 = 0$), the general solution of Eq.(9) is

$$D_{0B}(\theta) = R(1 + c_1\sin\theta + c_2\cos\theta). \quad (12)$$

The continuity of D and $\frac{dD}{dl} = (1 + \frac{x}{\rho})^{-1}D'$, combined with the symmetry condition $D'_{0Q} = 0$ at the center of the quadrupoles, can be solved to get

$$c_1 = \frac{c_2}{Q} = -\frac{Q}{(1+Q^2)\cos\frac{\theta_0}{2}}. \quad (13)$$

where $Q = Rq = \frac{s}{\theta_0} = \frac{Ns}{\pi}$. Subtituting Eq.(12) into Eq.(8) and Eq.(2) gives

$$\alpha_0 = \frac{1}{\theta_0}\int_{-\frac{\theta_0}{2}}^{+\frac{\theta_0}{2}} d\theta\frac{D_{0B}}{R} = 1 - \frac{2tQ^2}{\theta_0(1+Q^2)}, \quad (14)$$

where $t = tan(\frac{\theta_0}{2})$, and the wiggling factor

$$w = \frac{\langle D_0'^2\rangle}{2\alpha_0} = \frac{Q^2\left[\theta_0(1+t^2)(1+Q^2) + 2t(1-Q^2)\right]}{4(1+Q^2)\left[\theta_0(1+Q^2) - 2tQ^2\right]}. \quad (15)$$

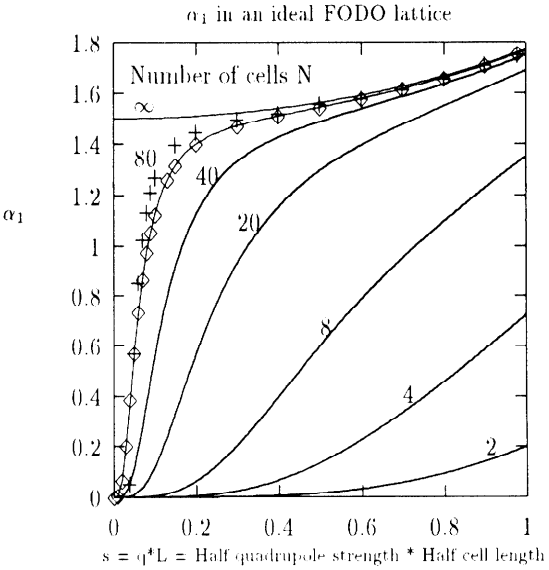

Figure 1: α_1 as a function of $s(\approx \sin\phi_{\frac{1}{2}})$ with different number of cells in an ideal FODO lattice. The solid line is the prediction from the analytical expression, which agrees excelently with MAD calculation with sector dipoles (diamond points). The plus points are MAD calculation with rectangular dipoles.

Following the same procedure, we now solve D_1. In the dipole

$$D_{1B}'' + \frac{1}{R^2}D_{1B} = -\frac{1}{R}(\frac{D_{0B}}{R} - 1)^2 + \frac{1}{R}\frac{D_{0B}'^2}{2} \quad (16)$$

with the general solution

$$D_{1B}(\theta) = R\left[c_3\sin\theta + c_4\cos\theta\right] - \frac{1}{2R}D_{0B}^2, \quad (17)$$

which leads to a very simple closed result

$$\alpha_0\alpha_1 = \frac{1}{\theta_0}\int_{-\frac{\theta_0}{2}}^{+\frac{\theta_0}{2}} d\theta(\frac{D_{1B}}{R} + \frac{1}{2R^2}D_{0B}^2) = c_4\frac{2\sin\frac{\theta_0}{2}}{\theta_0}. \quad (18)$$

c_4 can be solved from the boundary conditions and substituted into Eq.(18) to get

$$\alpha_0\alpha_1 = \frac{Q^4 t(Q^2t^2+3)}{\theta_0(1+Q^2)^3}. \quad (19)$$

Further substitution of Eq.(14) into Eq.(19) allows one to write

$$\alpha_1 = \frac{Q^4 t(Q^2t^2+3)}{(1+Q^2)^2\left[\theta_0(1+Q^2) - 2tQ^2\right]}, \quad (20)$$

which could alternatively be expressed as a function of s

$$\alpha_1 = \frac{s^4 t(s^2t^2 + 3\theta_0^2)}{(\theta_0^2+s^2)^2\left[\theta_0(\theta_0^2+s^2) - 2ts^2\right]}. \quad (21)$$

This result was also independently reached through a geometric approach[9].

Notice that both w and α_1 only depend on the strength of the quadrupoles and the number of cells. Fig. 1 is a plot of α_1 as a function of s with different number of cells. For a given N, w and α_1 increase as quadrupoles become stronger. The possible value of s is somewhere between 0 and 1 since $s \approx \sin\phi_{\frac{1}{2}}$. In the case $s = 0$ (cyclotron), from Eq. (14) and Eq. (20) we have $\alpha_0 = 1$ and $\alpha_1 = 0$ as expected. For real synchrotrons $\phi_{\frac{1}{2}}$ is usually between 30 and 45 degrees, and the operating range for s is $0.5 \sim 0.7$. Also notice that w and α_1 increase with N. Since N increases as ring size (roughly $N \propto \sqrt{R}$), w and α_1 are bigger for larger machines.

In the case $N \to \infty$, the centrifugal focussing of dipoles becomes negligible, and the analytical results reduce to

$$\alpha_0 = \frac{1}{Q^2}\left(1 - \frac{s^2}{12}\right), \tag{22}$$

$$\alpha_1 = 3w = \frac{3(1+\frac{s^2}{12})}{2\left(1-\frac{s^2}{12}\right)}. \tag{23}$$

5 Comparison With MAD

In general, the differential equations cannot be solved analytically and numerical method has to be used. Unfortunately, α_1 is not directly available from the general codes such as MAD [10], which instead return the momentum compaction factor α_p. The value of α_1 has to be extracted from the dependence of α_p on δ. Care must be taken about which definition of α_p is used in a specific code. It may be

$$\alpha_{p1} = \frac{p}{C}\frac{dC}{dp} = \alpha_0\left[1 + 2(\alpha_1 + \frac{1}{2} - \frac{1}{2}\alpha_0)\delta\right] + O(\delta^2), \tag{24}$$

or

$$\alpha_{p2} = \frac{p_s}{C_s}\frac{dC}{dp} = \alpha_0(1 + 2\alpha_1\delta) + O(\delta^2), \tag{25}$$

or something else. It is also important to test these codes using some very simple lattices, for which an analytical solution is possible. If there is a good agreement, we can have confidence in numerical solutions of realistic lattices such as the Main Ring or the Main Injector, or an isochronous ring.

A lattice composed of 80 simplified FODO cells was set up as input to MAD. The length of a quadrupole was chosen as 1 micron. For every s, the momentum compaction factor α_p is calculated by MAD at three momentum offsets $\delta = -\delta_t, 0, +\delta_t$ with $\delta_t = 0.001$. Then α_1 was extracted from α_p as

$$\alpha_1 = \frac{\alpha_{p2}(\delta_t) - \alpha_{p2}(-\delta_t)}{4\alpha_0\delta_t}, \tag{26}$$

if $\alpha_p = \alpha_{p2}$. The excellent agreement is achieved using the second definition, as shown in Fig. 1. The systematic discrepancy found in ref. [11] is now understood.

6 Deviation From the Ideal FODO Lattice

Taking the Main Injector ($N = 80, s = \sin\frac{\pi}{4} = \frac{1}{\sqrt{2}}$[12], so $N \to \infty$ approximation valid) as an example, we will see how the deviations from an ideal FODO lattice affect α_1.

Sector Dipoles and Rectangular Dipoles: In the ideal lattice we assumed there was no dipole edge focussing, as with sector dipoles. In reality the Main Injector dipole is rectangular. How important is this? Fig. 1 shows that the difference between sector dipoles and rectangular dipoles is negligible in the case of Main Injector. But as the cell phase advance and/or number of cells decreases the edge focussing becomes more important. So special care has to be taken with edge focussing in small accelerator rings.

Finite Length Quadrupole: For the simplicity of analytical solution, we have used a thin quadrupole approximation. What happens if quadrupole has finite length? From the model lattice, we see that α_1 changes from 1.545 to 1.550 by increasing the quadrupole length from 2 micron to 1 meter. This is not a surprise because the dominant source of momentum compaction comes from dispersion in dipoles, and the boundary conditions are dominated by the integrated strength of the quadrupoles.

Contribution from Sextupoles: If the sextupole strengths are set to make the net chromaticity $(1 - f)$ times the natural chromaticity, D_0 (and thus α_0 and w) will not change while D_1 will be modified, as shown in [11]

$$\langle D_1\rangle \approx \frac{R}{Q^2}\left(1 - f + \frac{s^2}{12}\right). \tag{27}$$

This approximation is true when the focussing from dipoles is negligible. Then

$$\alpha_1 = \frac{3 - 2f + \frac{s^2}{4}}{2\left(1 - \frac{s^2}{12}\right)}. \tag{28}$$

So, when the net chromaticity is compensated to zero, or $f = 1$, $0.5 \le \alpha_1 = \frac{1+\frac{s^2}{4}}{2\left(1-\frac{s^2}{12}\right)} \le .68$, because $0 \le s \le 1$. For the Main Injector $s^2 = 0.5$, and we have $\alpha_1 = 0.587$. A value of $\alpha_1 = -1.5$ can be obtained in principle by setting $f \approx 3$ resulting in unpleasantly strong nonlinear fields.

Acknowledgements

The possible importance of the previously neglected wiggling factor was first pointed out to us by Leo Michelotti. We thank K.Y. Ng for his help in the discussion of differential equations. Discussions with W. Gabella were also very fruitful. Thanks also go to C. Ankenbrandt for his comments.

References

[1] K. Johnsen. In *Proc. of the CERN Symposium on High Energy Accelerators and Pion Physics*, pages 106–109, CERN, 1956.

[2] D.A.G. Deacon. *Physics Report*, 76(5):349–391, 1981.

[3] S. Chattopadhyay et al. In *Proceedings of ICFA workshop on low emittance e^-e^+ beams*, BNL 52090, 1987.

[4] C. Pellegrini and D. Robin. *Nucl.Instr.and Meth. A*, 301:27–36, 1991.

[5] Bruck et al. *IEEE Trans. Nul.*, 20(3):822, June 1973.

[6] J.P. Shan, S. Peggs, and S. Bogacz. Fermilab pub92/124, April 1992.

[7] E. Ciapala, A Hofmann, S. Myers, and T. Risselada. *IEEE Nul.*, 26(3), June 1979.

[8] J.-P. Delahaye and J. Jager. *Particle Accelerators*, 18:183–201, 1986.

[9] K.Y. Ng. Fermilab FN 578, December 1991.

[10] H. Grote and F.C. Iselin. *The MAD Program(Methodical Accelerator Design). User's Reference Manual*. CERN, 8.1 edition, September 1990.

[11] S.A. Bogacz and S. G. Peggs. In *Proceedings of the Fermilab III Instabilities Workshop*, pages 192–206, Fermilab, June 1990.

[12] Fermilab main injector. Conceptual design report revision 2.3, appendum, Fermilab, March 1991.